Novel Titanium Carbide (Ti3C2Tx) MXene electrocatalyst for HER application.

Muhammad Yameen Solangi[1*], Abdul Hanan[2], Umair Aftab[1], Imtiaz Ali Soomro[1], Zafar Hussain Ibupoto[3],

[1]Department of Metallurgy and Materials Engineering, Mehran University of Engineering and Technology, 76080 Jamshoro, Sindh, Pakistan
[2]Sunway Centre for electrochemical energy and sustainable technology (SCEEST), School of Engineering and Technology, Sunway University, Selangor, Malaysia
[3]Dr. M.A Kazi Institute of Chemistry University of Sindh Jamshoro, 76080, Sindh, Pakistan
Corresponding Authorl: yameen.engineer14@gmail.com
Received: 21-11-2024, Received in Revised form: 08-03-2025, Accepted: 11-05-2025, Published: 30-06-2025

Abstract

Water electrolysis is a promising method for producing green hydrogen (H_2), and two-dimensional (2D) materials are gaining more attention globally, especially in the field of energy conversion/storage devices, because of their special attributes. The goal of this research is to create an electrocatalyst that is cost-effective, long-lasting, and sustainable using two-dimensional (2D) MXene materials from MAX phase. This study emphasized the synthesis of Ti3C2Tx based MXene via etching method. The surface morphology, elemental analysis, surface functionalization, crystalline phase purity, and water splitting behavior of the as-prepared catalyst (Ti_3C_2Tx) has been examined by numerous characterization techniques, including scanning electron microscopy (SEM), Energy dispersive spectroscopy (EDS), Fourier transform infrared spectroscopy (FTIR), X-ray diffraction (XRD), and electrochemical measurement. The robust 2D material (Ti_3C_2Tx) is found to have more effective hydrogen evolution reaction (HER) activity in 1.0 M KOH alkaline media. The electrocatalyst exhibits rapid reaction kinetics having an overpotential of 542 mV at a current density of 10 mA/cm2 accompanied with 170 mV/dec Tafel slope value. Additionally, as demonstrated by effective HER activity, it provides low charge transfer resistance (Rct) together with good stability, high electrochemical active surface area (ECSA), and durability for several hours. Moreover, Ti3C2Tx has superior turnover frequency and theoretical hydrogen production. Henceforth, for industrial-scale energy conversion systems, this innovative electrocatalyst may help to replace those electrocatalyst based on precious metals.

Keywords: Water splitting, Electrocatalyst, Hydrogen evolution reaction, 2D MXene, Alkaline Media

Introduction

The global demand for energy is rising alongside the growing population, leading to an anticipated increase in annual per capita consumption as human lifestyles advance [1-3]. Currently, 80% of the world's energy is derived from fossil fuels, which significantly harm the atmosphere by emitting greenhouse gases, thereby affecting the climate, raising Earth's temperature, and depleting freshwater resources [4]. There is a pressing need to develop more efficient and cost-effective renewable energy sources [5]. Hydrogen (H_2) technologies are gaining traction as a renewable energy option, with H_2 being produced through methods such as steam reforming, thermal decomposition, biomass fermentation, and electrolysis [6-8]. Among these, water electrolysis is particularly appealing because it generates H_2 by splitting water molecules into hydrogen and oxygen (O_2). During this process, two reactions occur: the hydrogen evolution reaction (HER) and the oxygen evolution reaction (OER) [9, 10]. The HER and OER take place at the cathode and anode in acidic and alkaline electrolytes, respectively. However, HER faces more challenges in alkaline environments, necessitating a higher electrical potential to proceed [11]. To address this, noble metal-based electrocatalysts like Platinum (Pt), Ruthenium (Ru), and Iridium (Ir) and their alloys are employed to facilitate the reaction at low overpotential [12]. Despite their effectiveness, these noble catalysts are expensive due to limited availability, making them less viable for large-scale production. Consequently, there is a global focus on developing new methods that are reliable for industrial-scale H_2 production [13]. In this context, two-dimensional (2D) materials have been developed and are widely used for energy storage and conversion applications [14]. Among these, MXene is a novel material known for its high electrical conductivity and adjustable surface functionality [15]. MXene is derived from the MAX phase, with the general formula $M_{n+1}AX_n$ (n = 1, 2, 3), where M represents transition metals, A denotes IIIA or IVA elements, and X indicates nitrogen or carbon [16, 17]. To produce MXene, the A layer (such as Al, Ga) is selectively removed and replaced with Tx functional groups (-O, -OH, and -F). $Ti_3C_2T_x$ MXene is predominantly used in H_2 generation applications due to its excellent metallic conductivity and hydrophilicity [18, 19]. Recent literature reports various thin-layered $Ti_3C_2T_x$ MXene electrocatalysts for HER activity, such as MoS_2/Ti_3C_2 [20], Fe/Ni doped GO@ $Ti_3C_2T_x$ [21], and1T/2H MoS_2 (25D)/ $Ti_3C_2T_x$-1 [22]. However, MXene nanosheets exhibit strong intermolecular attraction, leading to restacking or reaggregation after dehydration, which significantly reduces the number of electrocatalytically active sites [23]. Therefore, it is crucial to develop combinations with MXene that preserve its thin-layered, delaminated structure.

This research presents a promising method for synthesizing $Ti_3C_2T_x$ using an acid etching technique, where $Ti_3C_2T_x$ is derived from Ti_3AlC_2 through the use of HCl and HF acids. Various physicochemical methods were employed to investigate the structural, compositional, and morphological properties. The newly synthesized catalyst, along with the MAX phase material, was evaluated for its HER activity in a 1.0 M KOH solution. The MXene demonstrated superior electrochemical performance, with an overpotential of 542 mV at a current density of 10 mA/cm^2, a Tafel slope of 170 mV/dec, and stability for 15 hours. This approach is entirely novel and has not been previously documented.

Experimental Works

MAX phase (Ti3AlC2), Hydrofluoric acid (HF), Potassium hydroxide (KOH), Hydrochloric acid (HCl), 5 wt% Nafion, and Deionized (DI) water were sourced from Sigma Aldrich in Karachi, Pakistan. The experiments utilized high-grade analytical materials without any purification.

The MXene was synthesized using an etching method involving HF and HCl. In this process, the Al layer was removed from the Ti_3AlC_2 MAX phase. Specifically, 0.5g of bulk MAX was gradually added to a Teflon-lined beaker

This work was presented at 4th ASEAN Pakistan Conference on Materials Science (APCOMS), 2025.

containing 60 mL of a solution made up of 20% aqueous hydrofluoric acid and 5% hydrochloric acid. The resulting Ti_3AlC_2 powder was continuously stirred at room temperature for 40 hours using a Teflon-coated magnetic stir bar. This led to the etching and removal of Al layers from the MAX phase. To neutralize the acidic nature of the solution, the HF acidic solutions were repeatedly centrifuged with deionized water until the pH reached approximately 7. The MXene was then collected and dried at room temperature. Consequently, the as-synthesized $Ti_3C_2T_x$ was prepared for characterization and optimization for electrochemical analysis.

To assess the phase purity and crystal orientation of the synthesized nanostructures, Philips PAN analytical X-ray diffraction techniques were employed. The equipment was set to operate at a voltage of 45 kV, a current of 45 mA, and utilized CuKa radiation with a wavelength of 1.5418 °A. The resulting X-ray spectra were analyzed using High Score Plus software. For morphological and elemental analysis of the synthesized materials, JEOL JSM-6480A Scanning Electron Microscopy (SEM)/ Energy Dispersive Spectroscopy (EDS) was conducted at an operating voltage of 20 kV. Additionally, the surface functionalization of the samples was examined through Fourier Transform Infrared (FTIR) Spectroscopy, via PerkinElmer's Spectrum two instrument. Each sample, with a concentration of 0.5 wt%, was mixed with dried KBr for measurement, and the operating range was maintained between 400 and 4000 cm^{-1}.

The electrochemical evaluation for the hydrogen evolution reaction (HER) was conducted using a VERSASTAT4-500 system equipped with a three-electrode cell setup. This setup included a reference electrode (silver/silver chloride), a counter electrode (platinum wire), a working electrode (glassy carbon electrode), and an electrolyte solution of 1.0 M KOH. The GCE was modified with catalyst ink, which was prepared by mixing 5 mg of the synthesized catalyst, 20 µL of a 5% Nafion solution, and 4 mL of deionized water. The mixture was thoroughly dispersed using an ultrasonic bath for 25 minutes. The resulting uniform ink was applied to the cleaned GCE surface and dried by blowing air. The dried GCE was then incorporated into the cell setup for electrochemical testing. The HER polarization curve was initiated using linear sweep voltammetry in 1.0 M KOH at a scan rate of 5 mV/s. To assess the durability of the optimal sample, a chrono-potentiometric test was conducted at current densities of 10 mA/cm² and 20 mA/cm² for 30 hours. Electrochemical impedance spectroscopy (EIS) was employed to analyze the charge transfer resistance (Rct) of the various synthesized catalysts, operating at -0.4 V vs RHE with a 5 mV sinusoidal potential across a frequency range from 100,000 Hz to 1 Hz. The electrochemical active surface area (ECSA) of the samples was determined using cyclic voltammetry (CV) at different scan rates in the non-faradaic region [24].

Results and discussion

Figure 2 illustrates the unique peak pattern of MAX powder (Ti3AlC2). The XRD patterns of the original MAX powder align well with the reference JCPDS no. 520-875, featuring both sharp and broad peaks at approximately 9.28°, 19.15°, 33.71°, 34.04°, 38.81°, 39.04°, 41.81°, 44.92°, 48.54°, 56.57°, and 60.25°, which correspond to the (002), (004), (100), (101), (008), (104), (105), (106), (107), (109), and (110) crystallographic planes [25, 26]. The XRD diffraction pattern of MXene reveals a prominent peak at 7.22° associated with the (002) plane, along with smaller peaks at 14.4° and 29° corresponding to the (004) and (006) planes, respectively, which are consistent with existing literature [27]. Following the HF+HCl exfoliation treatment, a significant shift in the (002) peak from 2θ 9.26° to 7.22° was observed, indicating an increase in the lattice parameter. The double contribution in single peak is also investigated and a zoomed-in XRD peaks analysis added as sub-figure2(b).

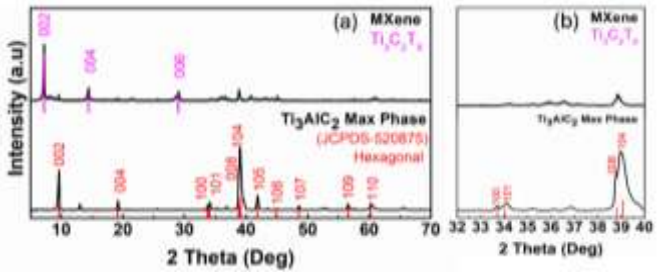

Figure 2. (a) XRD diffraction patterns of MAX Phase and MXene (b) Zoomed-in XRD peaks analysis

SEM analysis was employed to examine the morphology and structural characteristics of Ti_3AlC_2 and exfoliated MXene. Figure 3a [28] illustrates the irregular surface and densely packed structure of the MAX phase. Following HF+HCl treatment of the MAX phase, the MXene exhibited a morphology resembling exfoliated flakes, as shown in Figure 3b [29]. Our successful synthesis of MXene was confirmed through SEM analysis, aligning with the literature provided. The EDS analysis was also performed for elemental analysis. The EDS spectra of MAX phase contain C, Al and Ti elements with 8.77, 16.52 and 74.71% mass percentage as given Figure 3a. While the EDS spectra of MXene comprises C, F, Al and Ti elements with 5.16, 9.96, 0.66 and 84.22% mass percentage mentioned in Figure 3b. It can be observed that the mass percentage of Al is reduced from 16.52 to 0.66 % in MXene which validates the leaching of Al from MAX phase.

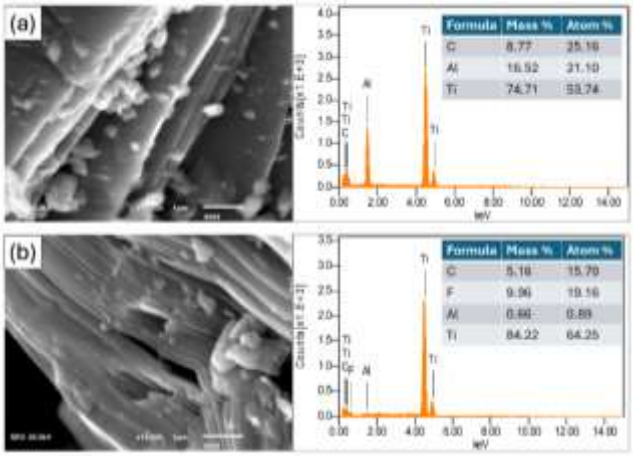

Figure 3. SEM micrographs and corresponding EDS spectra: (a) Ti3AlC2 (MAX) and (b) Ti3C2Tx (MXene)

FTIR spectroscopy was employed to examine the surface functionalization of the synthesized materials. Figure 4 displays the FTIR spectra for Ti_3AlC_2 (MAX) and $Ti_3C_2T_x$ (MXene). It was noted that all the materials exhibited

several common bands, specifically at 1382, 1601, 2854, 2930, and 3438, cm^{-1}, which correspond to (C-H), (O-H), (C-H), (C-H), and (O-H), respectively. The O-H groups are present due to the absorption of external water (H_2O) molecules on the material surfaces, attributed to their hydrophilic nature. The C-H bands in the materials are linked to the symmetrical/asymmetrical stretching of methylene (CH_2) and methyl (CH_3) groups [29, 30]. Additionally, the FTIR spectra of the Ti_3AlC_2 phase likely indicate Ti- Ti-O and O-Ti deformation vibration bonding at 605 and 879 cm^{-1}, respectively. Furthermore, the peaks at 481 cm^{-1} are indicative of the twisting vibration of Ti-C. In contrast, the $Ti_3C_2T_x$ exhibited a fluorine-terminated band (C-F) at 1108 cm^{-1} and a pronounced Ti-C band, confirming the etching of the Ti_3AlC_2 MAX phase.

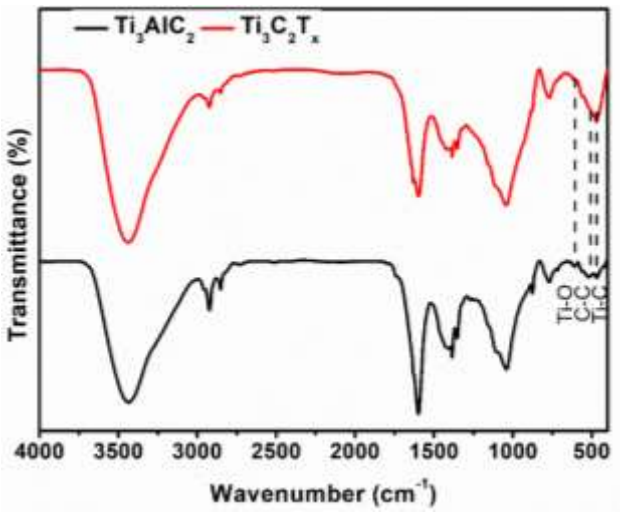

Figure 4. FTIR spectrum of Ti3AlC2 , and Ti3C2Tx

The electrochemical evaluation of Ti_3AlC_2 and $Ti_3C_2T_x$ is depicted in Figure 5. These electrocatalysts were subjected to HER analysis using LSV in a 1.0 KOH media, as illustrated in Figure 5(a). The LSV curve indicates that the $Ti_3C_2T_x$ exhibits an overpotential of 542 mV, while Ti_3AlC_2 shows a higher overpotential of 676 mV at 10 mA/cm^2 current density. The overpotential values for each catalyst are displayed in a histogram in Figure 5(b). The correlation between reaction rate and applied overpotential provides insights into the electrocatalysts' electrochemical performance, as indicated by the Tafel slope in Figure 5(c). The Tafel slopes for Ti_3AlC_2 and $Ti_3C_2T_x$ are 214 and 170 mV/dec, respectively. In an alkaline setting, the HER reaction kinetics are described by three sequential steps reported in literature [31-33].

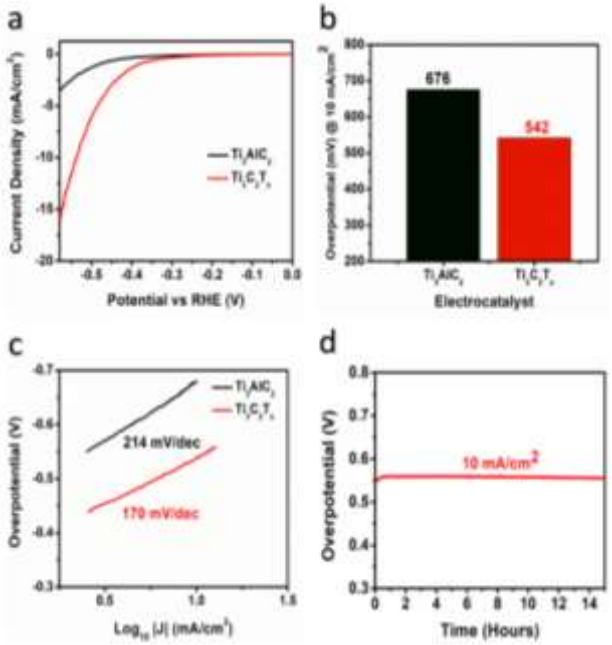

Figure 5. (a) LSV of different catalyst (b) Histogram of overpotentials of catalysts (c) Tafel slope values (d) Chronopotentiometric durability.

The durability of the MXene electrocatalyst has been assessed through the chronopotentiometry test, as depicted in Figure 5(d). The durability of an electrocatalyst is crucial for practical applications [34]. Therefore, the MXene material's stability was evaluated using chronopotentiometry at a current density of 10 over a period of 15 hours, confirming its extended-period electrochemical performance. It is important to note that the anticipated electrocatalyst has shown stability, as illustrated in Figure 5(e).

EIS has been carried to evaluate the charge transfer resistance (Rct) of different electrocatalysts in a 1 M KOH electrolyte. Figure 6 (a) illustrates the Nyquist and Bode (I and II) plots. When compared to MAX (Ti_3AlC_2), MXene ($Ti_3C_2T_x$) shows an enhanced phase angle in Figure 6 (a). Furthermore, the Rct values for Ti_3AlC_2 and $Ti_3C_2T_x$ have been determined to be 2825 and 1705 Ω, respectively. As indicated in Table.1, MXene's lower Rct suggests superior electrical conductivity, which enhances its electrochemical performance relative to its counterparts.

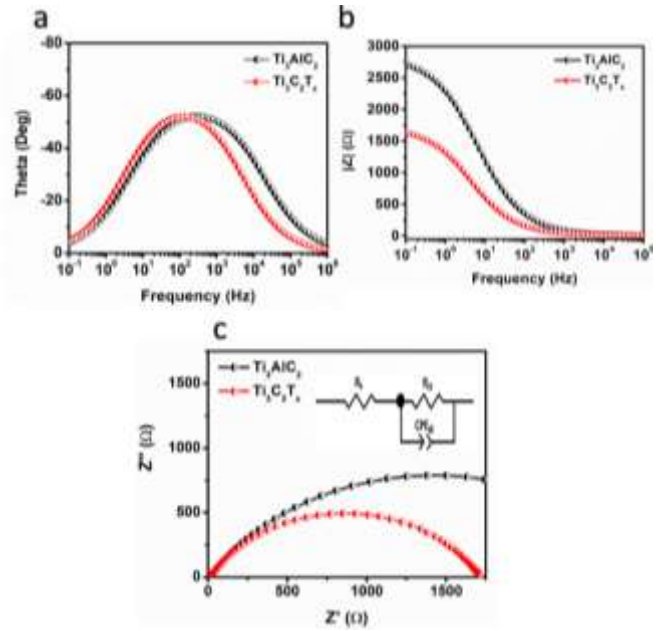

Figure 6. EIS data of Ti_3AlC_2, and $Ti_3C_2T_x$ showing (a &b) Bode plot and (c) Nyquist plot.

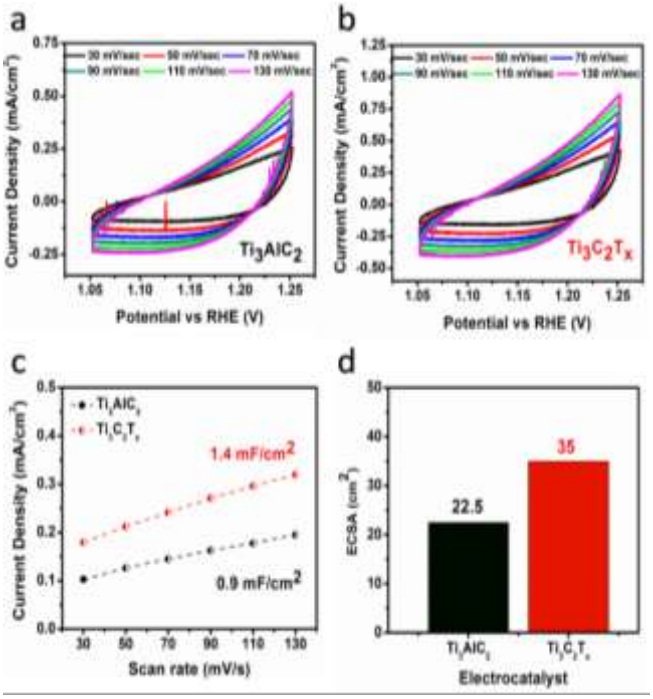

Figure 7. CV data (a, & b) of catalyst (c) C_{dl} data of prepared catalyst (d) ECSA calculated from C_{dl}.

Additionally, cyclic voltammetry (CV) has been applied to examine the double-layer capacitance (Cdl) in the non-faradic region of the synthesized electrocatalyst, as illustrated in Figure 7 (a & b). This analysis utilized various scan rates, specifically 30, 50, 70, 90, 110, and 130 mV/s. The calculated Cdl values are 0.9 and 1.4 μF/cm^2 for Ti_3AlC_2 and $Ti_3C_2T_x$, respectively, as represented in Figure 7 (c). Furthermore, the electrochemical active surface area (ECSA) was determined using the Cdl values through the formula provided.

$$ECSA=Cdl/Cs \quad (4)$$

In equation (4), Cdl denotes the double-layer capacitance, whereas Cs refers to the specific capacitance at the electrolyte interface. It is important to note that the Cs value is 0.04 mF/cm^2 for 1 M KOH media. The ECSA values for $Ti_3C_2T_x$ and Ti_3AlC_2 have been calculated as 35 and 22.5 cm^2, respectively, as shown in Figure 7(d). The comparative analysis with literature is given in Table. 2.

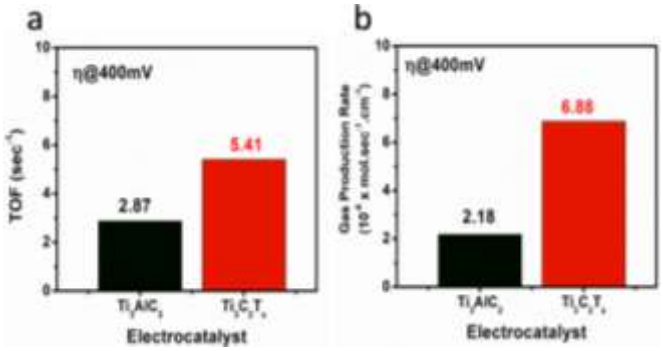

Figure 8. (a) Turnover Frequency at 400 mV overpotential (c) H_2 production @ fixed 400 mV overpotential

The turnover frequency (TOF) for different electrocatalysts is determined at a constant overpotential of 400 mV, as illustrated in Figure 8 (a). The current densities and corresponding TOFs for $Ti_3C_2T_x$ and Ti_3AlC_2 are 1.32 mA/cm^2 and 5.41 s^{-1}, and 0.42 mA/cm^2 and 2.87 s^{-1}, respectively. This suggests that CT-30 has the potential to significantly excel in industrial applications. To support this, theoretical H_2 production is also calculated to confirm the electrocatalyst's gas production rate.

Figure 8 (b) illustrates the hydrogen gas production rates for different catalysts. The findings indicate that MXene achieves a superior hydrogen production rate of 6.88x10^{-6} mol/s.cm compared to the others. This enhancement likely boosts the performance of this composition, making it a promising candidate for HER activity in KOH media. Table.1 presents various electrochemical characteristics of the prepared materials. In summary, MXene demonstrated strong electrochemical performance, aligning with recent research findings.

Table I
Concise features of prepared catalysts for HER application.

Catalyst	LSV data		EIS data		CV data	
	Overpotential	Tafel Slope	Charge Transfer Resistance	Double Layer Capacitance	Double Layer Capacitance	Electrochemically active surface area
	η_{10} (mV)	B (mV/dec)	R_{ct} (Ω)	CPE_{dl} (mF)	C_{dl} (μF/cm^2)	ECSA (cm^2)
Ti_3AlC_2	676	214	2825	0.01	0.9	22.5
$Ti_3C_2T_x$	542	170	1705	0.03	1.4	35

Table II
Comparative Analysis with Literature

Catalyst	R_{ct} *(Ω)*	ECSA *(cm^2)*	References
$Ti_3C_2T_x$	30.04	2.31	[35]
$Ti_3C_2T_x$	512	72.5	[36]
$Ti_3C_2T_x$	1705	35	This Work

5. Conclusion

To conclude, the electrocatalysts discussed were successfully created using an aqueous chemical growth technique. The two-dimensional material $Ti_3C_2T_x$ was synthesized with success. The physical and electrochemical properties of the synthesized material, along with its MAX phase, were examined using numerous analytical methods. MXene demonstrated a lower overpotential of 542 mV at 10 mA/cm^2 current density compared to the MAX sample in an alkaline electrolyte. Furthermore, the low Tafel slope of MXene, approximately 170 mV/dec, further enhanced its HER activity. It was observed that the MXene catalyst remained durable and stable at a current density of 10 mA/cm^2 for 15 hours without any potential drop. The 2D structure of $Ti_3C_2T_x$ facilitated easy charge carriage, resulting in a low charge transfer resistance (Rct) of 1705 Ω, a higher double layer capacitance (Cdl) of 1.4 μF/cm^2, and a greater electrochemical active surface area (ECSA) of 35 cm^2. Consequently, this enhances the sturdiness of the hydrogen evolution reaction (HER), which is advantageous for energy production applications.

Author Contributions

Muhammad Yameen Solangi, prepared desired material, analyzed initial HER test, and written part of the manuscript, Abdul Hanan investigated physical tests FTIR and written his part, Imtiaz Ali Soomro written the manuscript part with some post characterizations such as Chronopotentiometry and other physical tests, Zafar Hussain investigated physical tests (SEM/EDS) and partially supervised the work, Umair Aftab overall supervised the work and written relevant part of the manuscript.

Acknowledgement

The authors would like to express their heartfelt gratitude to the department of Metallurgy & Materials Engineering, Mehran University of Engineering & Technology, Jamshoro.

Conflicts of Interest

The authors of this paper have acknowledged no conflicts of interest.

References

1. R. Badrnezhad, et al., "Effect of iron on Ni–Mo–Fe composite as a low-cost bifunctional electrocatalyst for overall water splitting", International Journal of Hydrogen Energy, Vol. 46, no. 5, pp. 3821-3832, 2021.
2. Y. A. Bhutto, et al., "Investigating the optical absorption and thermal conductivity of nano-enhanced lauric acid phase change material for energy storage application", in IOP Conference Series: Earth and Environmental Science, 2023. IOP Publishing.
3. Y. A. Bhutto, et al., "Thermal behaviour of Paraffin-MWCNT stabilized by Sodium dodecylbenzene sulphonate nano-enhanced phase change material for energy storage applications", in IOP Conference Series: Earth and Environmental Science, 2023. IOP Publishing.
4. A. Islam, et al., "Shape stable composite phase change material with improved thermal conductivity for electrical-to-thermal energy conversion and storage", Materials Today Sustainability, Vol. 25, p. 100678, 2024.
5. Y. A. Ali Bhutto, et al., "Electrical and thermal performance assessment of photovoltaic thermal system integrated with organic phase change material", 2024, Vol. 488, p. 01007.
6. U. Aftab, et al., "Mixed CoS2@Co3O4 composite material: An efficient nonprecious electrocatalyst for hydrogen evolution reaction", International Journal of Hydrogen Energy, Vol. 45, no. 27, pp. 13805-13813, 2020.
7. A. Hanan, et al., "Co2FeO4@ rGO composite: Towards trifunctional water splitting in alkaline media", 2022, Vol. 47, no. 80, pp. 33919-33937.
8. A. Pareek, et al., "Insights into renewable hydrogen energy: Recent advances and prospects", Materials Science for Energy Technologies, Vol. 3, pp. 319-327, 2020.
9. A. J. Laghari, et al., "MgO as promoter for electrocatalytic activities of Co3O4–MgO composite via abundant oxygen vacancies and Co2+ ions towards oxygen evolution reaction", International Journal of Hydrogen Energy, Vol. 48, no. 34, pp. 12672-12682, 2023.
10. P. Banoth, C. Kandula, and P. Kollu, "Introduction to Electrocatalysts", in Noble Metal-Free Electrocatalysts: New Trends in Electrocatalysts for Energy Applications. Volume 2. American Chemical Society, pp. 1-37, 2022.
11. Z. H. Ibupoto, et al., "NiCo2O4 nanostructures loaded onto pencil graphite rod: An advanced composite material for oxygen evolution reaction", 2022, Vol. 47, no. 10, pp. 6650-6665.
12. W. Li, et al., "Defective RuO2/TiO2 nano-heterostructure advances hydrogen production by electrochemical water splitting", Chemical Engineering Journal, Vol. 431, p. 134072, 2022.
13. N. T. T. Thao, et al., "Current Trends of Iridium-Based Catalysts for Oxygen Evolution Reaction in

Acidic Water Electrolysis", 2024, Vol. 4, no. 1, p. 2300109.
14. L. Zhang, et al., "Manganese–cobalt hydroxide nanosheets anchored on a hollow sulfur-doped bimetallic MOF for high-performance supercapacitors and the hydrogen evolution reaction in alkaline media", Dalton Transactions, Vol. 53, no. 3, pp. 1274-1283, 2024.
15. A. Hanan, et al., "Novel rGO@Fe3O4 nanostructures: An active electrocatalyst for hydrogen evolution reaction in alkaline media", Journal of the Indian Chemical Society, Vol. 99, no. 5, p. 100442, 2022.
16. M. Rahman and M. S. Al Mamun, "Future prospects of MXenes: synthesis, functionalization, properties, and application in field effect transistors", Nanoscale Advances, Vol. 6, no. 2, pp. 367-385, 2024.
17. S. B. Devi and R. Navamathavan, "One-Pot Hydrothermal Synthesis of Ti3C2 (MXene)-CoS2 Nanocomposite as a Bifunctional Electrocatalyst (HER/OER) for a Clean Environment", Journal of the Electrochemical Society, Vol. 170, no. 9, 2023.
18. D. Liu, et al., "Nitrogen-Doped MoS2/Ti3C2TX Heterostructures as Ultra-Efficient Alkaline HER Electrocatalysts", Inorganic Chemistry, Vol. 60, no. 13, pp. 9932-9940, 2021.
19. L. P. Hao, et al., "Synergistic Integration of MXene and Metal-Organic Frameworks for Enhanced Electrocatalytic Hydrogen Evolution in an Alkaline Environment", 2023, Vol. 13, no. 5, p. 802.
20. S. K. Raj, et al., "Three-dimensional Ni/Fe doped graphene oxide @ MXene architecture as an efficient water splitting electrocatalyst", International Journal of Hydrogen Energy, Vol. 47, no. 99, pp. 41772-41782, 2022.
21. J. Y. Loh, F. M. Yap, and W. J. Ong, "2D/2D heterojunction interface: Engineering of 1T/2H MoS2 coupled with Ti3C2Tx heterostructured electrocatalysts for pH-universal hydrogen evolution", Journal of Materials Science & Technology, Vol. 179, pp. 86-97, 2024.
22. Attanayake, et al., "Vertically aligned MoS$_2$ on Ti$_3$C$_2$ (MXene) as an improved HER catalyst", Journal of Materials Chemistry A, Vol. 6, no. 35, pp. 16882-16889, 2018.
23. Z. Z. Xu, et al., "Facile fabrication of carbon fiber skeleton structure of MoS$_2$ supported on 2D MXene composite with highly efficient and stable hydrogen evolution reaction", Composites Science and Technology, Vol. 222, 2022.
24. M. Y. Solangi, et al., "In-situ growth of nonstoichiometric CrO0.87 and Co3O4 hybrid system for the enhanced electrocatalytic water splitting in alkaline media", International Journal of Hydrogen Energy, 2023.
25. Z. Mahmoudi, et al., "Synthesis of Ti2AlC & Ti3AlC2 MAX phases by Arc-PVD using Ti–Al target in C_2H_2/Ar gas mixture and subsequent annealing", Ceramics International, Vol. 46, no. 4, pp. 4968-4975, 2020.
26. V. I. Vershinnikov and D. Y. Kovalev, "Preparation of Ti2AlC and Ti3AlC2 MAX Phases by Self-Propagating High-Temperature Synthesis with the Reduction Stage", Russian Journal of Non-Ferrous Metals, Vol. 61, no. 5, pp. 554-558, 2020.
27. R. R. Raja Sulaiman, et al., "Structurally modified MXenes-based catalysts for application in hydrogen evolution reaction: a review", 2022, Vol. 12, no. 12, p. 1576.
28. S. Munir, et al., "Exploring the Influence of Critical Parameters for the Effective Synthesis of High-Quality 2D MXene", ACS Omega, Vol. 5, no. 41, pp. 26845-26854, 2020.
29. X. Li, et al., "Advances in MXene Films: Synthesis, Assembly, and Applications", Transactions of Tianjin University, Vol. 27, no. 3, pp. 217-247, 2021.
30. N. U. Kiran, et al., "Comparative Study of Cold Electron Emission from 2D Ti3C2TX MXene Nanosheets with Respect to Its Precursor Ti3SiC2 MAX Phase", ACS Applied Electronic Materials, Vol. 4, no. 6, pp. 2656-2666, 2022.
31. S. Tang, et al., "Recent advances in transition metal nitrides for hydrogen electrocatalysis in alkaline media: From catalyst design to application", Front Chem, Vol. 10, p. 1073175, 2022.
32. S. Pakhira, V. Kumar, and S. Ghosh, "Revealing the Superior Electrocatalytic Performance of 2D Monolayer WSe2 Transition Metal Dichalcogenide for Efficient H_2 Evolution Reaction", 2023, Vol. 10, no. 8, p. 2202075.
33. A. Kazemi, F. Manteghi, and Z. Tehrani, "Metal Electrocatalysts for Hydrogen Production in Water Splitting", ACS Omega, Vol. 9, no. 7, pp. 7310-7335, 2024.
34. R. A. Mir, S. Upadhyay, and O. P. Pandey, "A review on recent advances and progress in Mo2C@C: A suitable and stable electrocatalyst for HER", International Journal of Hydrogen Energy, Vol. 48, no. 35, pp. 13044-13067, 2023.
35. X. Li, Y. Guo, Y. Li, and R. Fu, “2D Ti3C2Tx MXene-Supported Graphitic Carbon-Nitride-Decorated Co3O4 Nanoparticles as Efficient Catalysts for Oxygen Evolution Reaction,” ACS Appl. Energy Mater., vol. 6, no. 11, pp. 5774–5786, Jun. 2023, doi: 10.1021/acsaem.3c00162.
36. A. Hanan et al., “MXene based electrocatalyst: CoS2@Ti3C2Tx composite for hydrogen evolution reaction in alkaline media,” Materials Today Sustainability, vol. 24, p. 100585, Dec. 2023, doi: 10.1016/j.mtsust.2023.100585.